Research paper

Difference in glycogen metabolism (glycogen synthesis and glycolysis) between normal and dysplastic/malignant oral epithelium

Hitoshi Aizawa, DDS[1], Shin-ichi Yamada[1,*], Tiepeng Xiao[2], Tetsu Shimane[1], Kiyonori Hayashi[1], Fanfang Qi[1], Hirokazu Tanaka[1], Hiroshi Kurita[1]

[1]Department of Dentistry and Oral Surgery, Shinshu University School of Medicine, 3-1-1 Asahi, Matsumoto 390-8621, Japan

[2]Department of Orthodontics, Second Hospital of Hebei Medical University, 050000 Shijiazhuang, China

[*]Corresponding author: Shin-ichi Yamada, DDS, PhD
Department of Dentistry and Oral Surgery
Shinshu University School of Medicine
3-1-1, Asahi, Matsumoto, 390-8621, Japan
Tel: +81 (0)263-37-2677, Fax: +81 (0)263-37-2676
E-mail: yshinshin@shinshu-u.ac.jp

Running title: Vital staining with iodine solution in OSCC

Abstract

Background: The purpose of this study was to investigate a difference in glycogen metabolism (glycogen synthesis and glycolysis) between the iodine stained (normal non-keartinized) and the unstained (dysplasctic/malignant) oral epithelium.

Methods: Twenty-one frozen tissue samples of iodine-stained and unstained mucosal tissue were obtained from 21 OSCC patients. Serial frozen sections were cut and examined with the hematoxylin-eosin and periodic acid-Schiff methods and immunohistochemical (IHC) staining for Ki67, P53, molecules associated with glycogenesis (i.e., glycogen synthase (GS) and phospho-glycogen synthase (PGS)), and molecules associated with glycogenolysis (i.e., glycogen phosphorylase isoenzyme BB (GPBB) examine the glycogen metabolism in OSCC. Additionally, *in vitro* study, the expression levels of GS and GPBB in the cultured cells were analyzed by immunofluorescent staining, Western blot analysis, and the real-time quantitative polymerase chain reaction (PCR).

Results: There was no significant difference in GS and PGS immunoactivity between iodine stained and unstained area. On the other hand, significantly greater GPBB immunoreactivity was observed in the basal and parabasal layers of iodine-unstained epithelium, where higher positivity for p53 and Ki67 was also showed. Additionally, western blot analysis, immunofluorescent staining, and real-time quantitative PCR revealed that the oral squamous cancer cells exhibited

greater expression of GPBB than normal epithelial cells.

Conclusions: The results of this study showed that GPBB expression, which resulted in up-regulation of glycogenolysis, is enhanced in oral dysplastic/malignant epithelium compared with non-keartinized normal epithelium, in spite of the fact that glycogenesis continues in both of them. Premalignant and malignant epithelial cells consume greater quantities of energy due to their increased proliferation, and hence, exhaust their glycogen stores, which resulting in negative stain reaction with iodine solution.

Keywords:

Oral squamous cell carcinoma (OSCC) • Glycogen metabolism • Iodine vital staining • Glycogen phosphorylase isoenzyme BB • Glycogen synthase

Introduction

Oral squamous cell carcinoma (OSCC) is the most common malignant tumor of the oral cavity (Jemal, Bray, & Center, 2011). During the treatment of OSCC, surgical margin status is an important prognostic factor for both recurrence and overall survival (Binahmed, Nason, & Abdoh, 2007; Kurita, Nakanishi, & Nishizawa, 2010; Xiao, Kurita & Shimane, 2013).To ensure a complete tumor resection is achieved, vital staining with iodine solution is widely used to discriminate between the normal and the dysplastic/malignant oral epithelium (Chisholm, Williams, & Leung, 1992; Epstein, Scully, &Spinelli, 1992; Kurita, & Kurashina, 1996; Ohta, Ogawa, & Ono, 2010). It is thought that the iodine reacts with glycogen existed in the cytoplasm of oral epithelium (Xiao, Kurita & Shimane, 2013). Iodine solution is retained in normal non-keratinized squamous epithelium, but not in severely dysplastic or malignant epithelial tissue, because of differences in the glycogen content of the cytoplasm between them (Nakanishi, Ochiai, & Shimoda, 1997; Dawsey, Fleischer, & Wang, 1998; Shimizu, Tsukagoshi, & Fujita, 2001; Xiao, Kurita & Shimane, 2013; Ogawa, Washio & Takahashi, 2014). The oral epithelium that exhibit dysplastic changes with a high potential for malignant transformation has been reported to contain reduced amounts of glycogen (Epstein, Scully, &Spinelli, 1992; Chisholm, Williams, & Leung, 1992; Xiao, Kurita & Shimane, 2013). It is well known that

glucose consumption is highly elevated in oral dyplastic/malignant epithelial cells. Glycogen is thought to be “a store of glucose” and may also be used up. However, little is known about glycogen metabolism (glycogen synthesis and glycolysis) in oral dysplastic/malignant epithelial cells (Xiao, Kurita & Shimane, 2013; Ogawa, Washio & Takahashi, 2014).

Therefore, the purpose of this study was to investigate a difference in glycogen metabolism (glycogen synthesis and glycolysis) between the iodine stained and the unstained oral epithelial tissue. We hypothesized that premalignant and malignant epithelial cells consume greater quantities of energy due to their increased proliferation, and hence, exhaust their glycogen stores.

Materials and methods

Patients

From June 2011 to September 2014, 55 consecutive patients with histologically proven primary OSCC were examined. Of these patients, 21 samples included both iodine stained and unstained area and were successfully subjected to frozen section analysis were included in this study. Written informed consent was obtained from all patients before their inclusion, and the study was approved by the ethics committee of the Shinshu University School of Medicine (No.1341).

Histology and immunohistochemistry

Dental iodine glycerin (10 mg iodine/100 ml; Showa Yakuhin, Japan) was used as the vital staining solution before the resection of the primary tumor. Iodine staining of the tissue around the lesion was performed as described by Kurita et al (Kurita & Kurashina, 1996). Specimens that included both iodine-stained and unstained areas were obtained from the boundary region (Fig. 1). All specimens were stored at -80°C after being snap-frozen in dry ice-cooled acetone (Xiao, Kurita & Shimane, 2013). Serial 5-μm frozen sections were cut and mounted on Matsunami adhesive silane-coated glass slides (Matsunami Glass, Japan). The first vital section was placed in xylene for 30 s after being subjected to 30 min air-drying at room temperature, and was then mounted onto a coverslip. These slides were subjected to light microscopic examinations and microphotography as soon as possible because the brown-black color of iodine can gradually disappear over the course of 2 weeks. The other sequential sections were subjected to hematoxylin and eosin (H&E) and periodic acid-Schiff (PAS) staining. To ensure optimal cell structure preservation and that the tissue remained sensitive to immunostaining, 20% formalin neutral buffer solution was used to fix the sections, which were then subjected to 12 min of microwave treatment in Tris/ethylenediamine tetraacetic acid (pH 8.0) for antigen retrieval. Normal serum blocking and exclusion of the primary antibody were used to produce negative controls. Immunoreactivity was visualized with diaminobenzidine and hydrogen peroxide (Xiao, Kurita & Shimane, 2013). The antibodies

used in this study included anti-p53 (malignant cell marker; 1:200 dilution; DO-7, Dako, Denmark), Ki67 (cell proliferation marker; 1:300 dilution; MIB-1, Dako, Denmark), glycogen synthase (GS) (glycogen synthesis marker; 1:100 dilution; 15B1, Cell Signaling Technology, Danvers, MA, USA), phospho-glycogen synthase (PGS) (glycogen synthesis marker; 1:100 dilution; Ser641, Cell Signaling Technology, Danvers, MA, USA), glycogen phosphorylase isoenzyme BB (GPBB) (glycolysis marker; 1:100 dilution; ab61036, Abcam, UK) and glucagon-like peptide-1 (GLP-1) (glycolysis marker; 1:2000 dilution; ab26278, Abcam, UK) antibodies.

In the assessment of histochemical studies, we divided the epithelium into three compartments: the basal, parabasal, and superficial layers, as described previously (Liu, Sauter, & Clapper, 1998). In addition, the superficial layer was divided into three equal parts (the upper, middle, and lower superficial layers), as described by Xiao et al.(Xiao, Kurita & Shimane, 2013) (Fig. 1). To investigate the difference on the expression level of the molecules (glycogenesis (i.e. GS and PGS) and glycogenolysis (i.e. GPBB)) between iodine-stained and ‐unstained epithelium, the percentages of cells that were positive for GS (membranous), PGS (membranous), and GPBB (membranous), and GLP-1 (membranous) in each layer were calculated in a 400× field (five fields per area), irrespective of the intensity of the staining. In each area, the first field was placed close to the boundary between the iodine-stained and unstained areas, and the other four fields were selected

randomly. All slides were reviewed and assessed by two independent observers, and the mean positive cell count was calculated (Xiao, Kurita & Shimane, 2013).

Cultured cell lines

Cells of the spontaneously immortalized human keratinocyte cell line HaCaT were obtained from Tohoku University. Normal human epithelial keratinocytes (NHEK) were isolated from normal oral mucosal tissue obtained from healthy volunteers. Both the HaCaT and NHEK cells were cultured in keratinocyte serum-free media (KSFM, Gibco, Cergy Pontoise, France) containing 0.09 mM calcium, supplemented with 25 mg/ml bovine extract (Gibco) and 1.5 ng/ml of recombinant epidermal growth factor (Gibco)(Koike, Yasuo, & Shimane, 2011).

Six cancer cell lines (SAS, HSC-2, HSC-3, SQUU-A, SQUU-B, and Ca9-22) derived from OSCC patients were also used. SAS, HSC-2, HSC-3, and Ca9-22 were obtained from the Japanese Collection of Research Bioresources. SQUU-A and SQUU-B were kindly donated by Kyushu University (Morifuji, Tniguchi, & Sakai, 2000). All of the OSCC cell lines were cultured in Eagles' medium (Nissui, Tokyo, Japan) supplemented with 10% heat-inactivated fetal bovine serum (Gibco). All of the cells were incubated at 37°C in a 5% CO_2 atmosphere. In all experiments, freshly trypsinized cells were seeded at a density of 4×10^4 cells/cm^2. For the preparation of samples following the molecular analyzes, the incubated cells were harvested at 90% confluent. The

expression levels of GS and GPBB in the cultured cells were analyzed by immunofluorescent staining, Western blot analysis, and the real-time quantitative polymerase chain reaction (PCR).

Cell immunofluorescent staining

In the immunofluorescence analysis, cells were cultured on coverslips, fixed with 0.4% paraformaldehyde for 20 min and then permeabilized with 0.1% Triton X 100 for 10 min at room temperature. After being incubated at 37°C for 30 min with blocking solution, the cells were incubated overnight at 4°C with primary antibodies against GS or GPBB and then incubated for 1 h at room temperature with Alexa Fluor 488 (diluted 1:400; Amersham Biosciences, Amersham, UK). Subsequently, the cells' nuclei were stained with 4′ 6-diamidino-2-phenylindole dihydrochloride (DAPI; Sigma-Aldrich, St. Louis, MO) for 10 min and then stored in the dark until they were evaluated. Finally, the stained cells were photographed with a confocal laser-scanning microscope (Leica TCS SP2 AOBS, Leica Microsystems, Tokyo, Japan). Primary antibodies against GS (diluted 1:100; Cell Signaling Technology, Danvers, MA, USA) and GPBB (diluted 1:100; Abcam, Cambridge, MA, USA) were used. All experiments were performed in triplicate.

Western blot analysis

In the Western blot analysis, 10 μg total proteins were separated using 12.5% sodium dodecyl

sulfate polyacrylamide gel electrophoresis (SDS-PAGE). The proteins were then transferred to polyvinylidene difluoride (PVDF) membranes (Millipore, Bedford, MA, USA), which were blocked with 5% skimmed milk for 1 h, before being incubated overnight at 4°C with each primary antibody. The primary antibodies against GS, GPBB, and mouse monoclonal anti-human β-actin (Sigma-Aldrich) were diluted 1:2000, 1:2000, and 1:5000, respectively. All blots were developed using Immobilon Western (Millipore Corporation, Billerica, MA, USA), according to the manufacturer's protocol. The membranes were submerged in Immobilon Western chemiluminescent horseradish peroxidase substrate (WBKLS0500, Millipore Corporation, Billerica, MA, USA) for 5 minutes and sealed in foil (David, Ciuraszkiewicz, & Someone, 2010).

Real-time quantitative PCR

Total RNA was extracted from the cells with an RNeasy mini kit (Qiagen, Valencia, CA, USA). Total RNA (100 ng) was reverse-transcribed with the PrimeScript RT reagent kit (Takara, Kusatsu, Shiga, Japan). The resultant cDNA products were analyzed using the Thermal Cycler Dice real-time polymerase chain reaction system (Takara, Kusatsu, Shiga, Japan) and SYBR Premix Ex Taq II (Takara, Kusatsu, Shiga, Japan). A reaction mixture containing cDNA, SYBR green, and primer mix (300 nm) was placed in each well of a 96-well plate. The reaction conditions were set at 95 °C for 3 min followed by 40 cycles of 95 °C for 15 s and 60 C for 30 s. The sequences of the primers are provided in Table 2. Other primers were designed using the software Genetyxever.7.0. The primers

were produced by Operon Technology (Tokyo, Japan) (Shimane, Kobayashi, & Takeoka, 2013)).

Statistics

The data were analyzed with GraphPad Prism (GraphPad Software, Inc., La Jolla, CA, USA) for Windows. Differences in the percentage of positive cells between the iodine-stained and unstained areas in each layer of the epithelium were assessed using the Wilcoxon signed-rank test. $P<0.05$ was considered to indicate a statistically significant difference.

Results

Iodine penetration and PAS reactions

The patients' characteristics are summarized in Table 1. The iodine-stained areas of the epithelium were characterized by a brown-black color, whereas the unstained areas were normal-colored. In the examination of the frozen sections, it was demonstrated that the iodine solution had gradually penetrated the tissue from the surface. The brown-black color did not reach the basal layer in any case (Fig. 2a).

The iodine-stained and unstained epithelial tissue regions were compared with the H&E-

and PAS-stained slides. In the H&E-stained sections, the difference between the atypical epithelium and normal epithelium was almost clear (Fig. 2b). Iodine-stained tissue was defined as normal non-keratinized epithelial tissue, while iodine-unstained tissue included OSCC and dysplasia according to WHO classification criteria (2005). In the PAS-stained sections, large numbers of glycogen granules were seen in the superficial layers of the iodine-positive areas (Fig. 2c). Glycogen granules were distributed throughout the superficial layers, but iodine was mainly observed in the upper third of the superficial layer. The PAS staining indicated that the distribution of glycogen was similar to that of iodine in the upper superficial layer.

Immunohistochemical study

Expressions of Ki67, p53, GS, PGS, and GPBB in histochemical staining were shown in Figures 2 and 3. GS and PGS staining were detected in both the basal and parabasal layers, and these molecules exhibited similar staining patterns in the iodine-positive and -negative epithelial tissue (Fig. 3a and 3c). On the other hand, Ki67, p53, and GPBB expression were observed in the iodine-negative epithelial tissue mainly in the basal and parabasal layers (Fig. 2d, 2e, and 3e). In contrast, no GLP-1 was detected in any specimen (Fig. 3g).

A statistical comparison between the GS positivity rates of the cells in the iodine-positive and -negative areas is shown in Figure 3b (iodine-positive vs. iodine-negative areas: basal layer, 83

vs. 93%; parabasal layer, 72 vs. 82%; superficial layer, 23 vs. 30%; Wilcoxon signed-rank test: not significant (NS)). A statistical comparison between the PGS positivity rates of the cells in the iodine-positive and -negative areas is shown in Figure 3d (iodine-positive vs. iodine-negative areas: basal layer, 91 vs. 94%; parabasal layer, 91 vs. 90%; superficial layer, 40 vs. 54%; Wilcoxon signed-rank test: NS). A statistical comparison between the GPBB positivity rates of the cells in the iodine-positive and -negative areas is shown in Figure 3f (iodine-positive vs. iodine-negative areas: basal layer, 60 vs. 88%; parabasal layer, 55 vs. 75%; superficial layer, 32 vs. 48%; Wilcoxon signed-rank test: $P<0.01$). Significant differences in GPBB expression were detected in all layers. The GPBB positivity rates of the iodine-negative areas were higher than those of the iodine-positive areas.

Cell immunofluorescent staining

Normal mucosa cells and OSCC cells were subjected to immunofluorescent staining of both GS and GPBB (Fig. 4). The GS expression observed in these cells is shown in Figure 4A ((a) NHEK, (b) HaCaT, (c) SAS, (d) HSC-2, (e) HSC-3, (f) SQUU-A, (g) SQUU-B, and (h) Ca9-22 cells), and their GPBB expression is shown in Figure 4B ((a) NHEK, (b) HaCaT, (c) SAS, (d) HSC-2, (e) HSC-3, (f) SQUU-A, (g) SQUU-B, and (h) Ca9-22 cells).

The results of the quantitative analysis of the fluorescence intensity (Alexa Fluor 488)

produced by the GS and GPBB antibodies, in which the Leica Confocal Software (LCS) was used for image processing and analysis, are shown in Figure 4C. The expression patterns of GS and GPBB observed in these experiments agreed with the immunohistochemical staining results. The distribution of GS in the normal cells coincided with that seen in the OSCC cell lines. In addition, GS staining resulted in similar fluorescence intensity in the normal and OSCC cells. On the other hand, the fluorescence intensity of GPBB was markedly higher in the OSCC cells than in the normal cells. In addition, immunofluorescent images revealed that GPBB was expressed at significant greater levels than GS in the OSCC cells (GS vs GPBB; Wilcoxon signed-rank test: NHEK:NS, all OSCC cell lines: $P<0.01$).

Western blot analysis and real-time quantitative PCR

The expression levels of GS and GPBB in 6 established OSCC cell lines (SAS, HSC-2, HSC-3, SQUU-A, SQUU-B, and Ca9-22) and normal keratinocytes (NHEK) were assessed by Western blotting and real-time quantitative PCR (Fig. 5). GS and GPBB expression were observed in most cell lines. However, stronger GPBB expression was seen in the cancer cell lines than in the NHEK. Real-time quantitative PCR revealed that although similar GS expression levels were seen in the normal and cancer cells, higher mRNA expression levels of GPBB in the 6 OSCC cell lines than in the NHEK (NHEK vs each OSCC cell lines; Wilcoxon signed-rank test: SAS, HSC-2, and HSC-3:

P<0.05, SQUU-A, SQUU-B, and Ca9-22: P<0.01).

Discussion

In the present study, all of the areas of normal epithelial tissue that were stained with iodine solution were PAS-positive, which indicated that parakeratotic epithelial tissue contains a large amount of glycogen. On the other hand, the unstained areas were PAS-negative, which suggested that the malignant/dysplastic epithelial tissue contained lower amounts of glycogen than the iodine-stained areas (Ohta, Ogawa, & Ono, 2010; Xiao, Kurita & Shimane, 2013). It is well known that iodine reacts with glycogen granules via the so-called iodine-starch reaction.

In the oral mucosa, marked glycogen storage is seen in normal non-keratinized epithelial tissue, and reduced glycogen storage is observed in dysplastic/malignant epithelial tissue. Some studies have reported a correlation between iodine retention and glycogen content in OSCC (Epstein, & Scully, 1992; Dawsey, Fleischer, & Wang, 1998).The mechanism of glycogen metabolism is summarized in Figure 6. Glycogenesis and glycogenolysis both occur in the cell cytoplasm. Glycogenesis starts with glucose entering the cell through the glucose transporter 1 (GLUT-1). Intracellular glucose is then converted to glucose 6-phosphate by hexokinase and isomerized to glucose 1-phosphate by phosphoglucomutase. Next, the glucose 1-phosphate is attached to a UDP molecule and bound to a glycogen molecule by GS (Ritterson, Guin, & Theodorescu, 2015).

Glycogenolysis involves the breakdown of polymeric glucose to monomeric glucose. Mature glycogen is generated from glucose 1-phosphate by glycogen phosphorylase, and glucose 1-phosphate can be converted back into glucose-6-phosphate by phosphoglucomutase. Glucose-6-phosphate cannot exit the cell. Instead, it is transported into the endoplasmic reticulum, where it is converted to glucose by glucose-6-phosphatase. Glucose then exits the cell through the GLUT-2 transporter (Yu, Ladapo, & Whitman, 1994; Zois, Favaro, & Harris, 2014).In this study, antibodies against GS and PGS were used to detect glycogenesis, and an antibody against GPBB was used to detect glycogenolysis.

GS is an enzyme that plays an important role in controlling glycogenesis. There are two main mammalian isoforms of GS, the muscular and hepatic isoforms (Browner, Nakano, & Bang, 1989; Bai, Zhang, & Werner, 1990).The muscular isoform of GS is expressed in several tissues (Roach, Cheng, & Huang, 1998).GS expression is regulated by multi-site phosphorylation. Phosphorylation tends to inactivate GS although its activity can be fully restored in the presence of glucose-6-phosphate, and hence, the glucose-6-phosphate activity ratio is used as an index of the activation state of the enzyme. PGS is one of the most important phosphorylation sites for the regulation of GS (Skurat, & Roach, 1995). In vivo (immunohistochemical studies) and in vitro analyses conducted in the present study, GS and PGS exhibited similar staining patterns in both the iodine-positive and -negative epithelial tissue. Thus, glycogenesis seems to occur at similar levels in

normal epithelial and oral dysplastic/malignant cells.

Glycogen phosphorylase (GP) is an enzyme that plays a key role in controlling glycogenolysis. It breaks glycogen down into glucose-1-phosphate in the first step of glycogenolysis. Three different GP isoenzymes have been recognized in humans, GP isoenzyme LL (GPLL), GP isoenzyme MM (GPMM), and GP isoenzyme BB (GPBB), which were named based on the tissues in which they were initially identified. Skeletal muscles solely contain GPMM; GPLL is present in all human tissues except the brain, heart, and skeletal muscles; and GPBB is mainly detected in the brain, but can also be found at high concentrations in cardiac muscle (Kato, Shimizu, & Kurobe, 1989; Newgard, Hwang, & Fletterick, 1989). In the presence of tissue hypoxia and ischemia, glycogenolysis is initiated by the conversion of GP into its more active form (Lee, Romero, & Dong, 2012). Tumor cells mainly generate energy by increasing glycolysis (as described by Warburg in the 1920s), which is the basis of positron emission tomography (PET) using the glucose analogue tracer fluorine-18 fluorodeoxyglucose (FDG) because most human cancers exhibit significantly increased glucose uptake (Gatenby, & Gillies, 2004). The facilitative glucose transport protein GLUT1 plays important roles in the FDG-PET imaging of human diseases. For example, in OSCC, GLUT1 overexpression was found to be useful for identifying candidates for FDG-PET (Carvalho, Cunha, & Rocha, 2011). Although glucose inflow is increased in cancer cells, a lack of glycogen is seen in the epithelium. In the results of this study, based on the difference in GPBB expression between

iodine-positive and -negative areas and between cultured normal and cancer cells lines, it can be stated that glycogenolysis is markedly upregulated in oral dysplastic/malignant cells compared with normal epithelial cells. Since, in the presence of hypoxia, conversion of GP into its more active form is initiated (Lee, Romero, & Dong, 2012), GPBB expression also may increase in such hypoxia condition. GLP-1 also plays a key role in glucose metabolism. GLP-1, which has been shown to have insulin-like effects, stimulates glycogen synthesis, GS activity, glucose oxidation and utilization, and inhibits glycogen phosphorylase activity. All of these processes contribute to regulating the physiological concentration of glucose (Green, Henriksen, & Pedersen, 2012). However, in this study, GLP-1 was not detected during the immunohistochemical study, and hence, we consider that it does not participate in glucose metabolism in OSCC. On the other hand, GPBB was detected in both the basal and parabasal layers, and similar pattern was observed in both p53 and Ki67 staining in the iodine–negative oral epithelium. These results suggested that glycogenolysis is activated in the basal and parabasal layers in the dysplastic/malignant oral epithelium, because of increased proliferation of malignant potential cells.

In conclusion, GPBB expression, which resulted in up-regulation of glycogenolysis, is enhanced in oral dysplastic/malignant epithelial cells compared with non-keartinized normal epithelial cells, in spite of the fact that glycogenesis continues in these cells. The results of this study suggest that glycogenolysis is activated in dysplastic/malignant oral epithelial tissue, and hence, such

tissue lacks glycogen, resulting in it being negatively stained with iodine solution. The limitation of this study was to evaluate the findings based on relatively small number of cases. Therefore, further investigation based on more large number of cases is needed.

Declarations

Funding: None.

Competing Interests: None.

Ethical Approval: This study was approved by the Committee on Medical Research of Shinshu University (No.1341).

Patient Consent: not required.

References

Bai, G., Zhang, ZJ., & Werner, R.(1990). The primary structure of rat liver glycogen synthase deduced by cDNA cloning. Absence of phosphorylation sites 1a and 1b. J Biol Chem, 265(14), 7843-7848.

Binahmed, A., Nason, RW., & Abdoh, AA.(2007). The clinical significance of the positive surgical margin in oral cancer. Oral Oncol, 43(8), 780-784.

Browner, MF., Nakano, K., & Bang, AG.(1989). Human muscle glycogen synthase cDNA sequence: a negatively charged protein with an asymmetric charge distribution. Proc Natl Acad Sci U S A ,86(5),1443-1447.

Carvalho, KC., Cunha, IW., & Rocha, RM.(2011). GLUT1 expression in malignant tumors and its use as an immunodiagnostic marker. Clinics (Sao Paulo), 66(6), 965-972.

Chisholm, EM., Williams, SR., & Leung, JW, et al. (1992). Lugol's iodine dye-enhanced endoscopy in patients with cancer of the esophagus and head and neck. Eur J Surg Oncol, 18(6),550-552.

David, R., Ciuraszkiewicz, A., & Simeone, X.(2010). Biochemical and functional properties of distinct nicotinic acetylcholine receptors in the superior cervical ganglion of mice with targeted deletions of nAChR subunit genes. Eur J Neurosci, 31(6), 978-993.

Dawsey, SM., Fleischer, DE., & Wang, GQ.(1998). Mucosal iodine staining improves endoscopic

visualization of squamous Linxian, China. Cancer, 83(2),220-231.

Epstein, JB., Scully, C., & Spinelli, J(1992). Toluidine blue and Lugol's iodine application in the assessment of oral malignant disease and lesions at risk of malignancy. J Oral Pathol Med, 21(4),160-163.

Gatenby, RA., & Gillies, RJ.(2004).Why do cancers have high aerobic glycolysis? Nat Rev Cancer, 4(11),891-899.

Green, CJ., Henriksen, TI., & Pedersen, BK. (2012). Glucagon Like Peptide-1-Induced Glucose Metabolism in Differentiated Human Muscle Satellite Cells Is Attenuated by Hyperglycemia. PLoS One, 7(8), e44284.

Jemal, A., Bray, F., & Center, MM.(2011). Global cancer statistics. CA Cancer J Clin, 61(2),69-90.

Kato, K., Shimizu, A., & Kurobe, N. (1989). Human brain-type glycogen phosphorylase: quantitative localization in human tissues determined with an immunoassay system. J Neurochem, 52(5),1425-1432.

Koike, T., Yasuo, M., & Shimane, T.(2011). Cultured epithelial grafting using human amniotic membrane: the potential for using human amniotic epithelial cells as a cultured oral epithelium sheet. Arch Oral Biol, 56(10),1170-1176.

Kurita, H., & Kurashina, K. (1996). Vital staining with iodine solution in delineating the border of oral dysplastic lesions. Oral Surg Oral Med Oral Pathol Oral Radiol Endod, 81(3), 275-280.

Kurita, H., Nakanishi, Y., & Nishizawa R, et al. Impact of different surgical margin conditions on local recurrence of oral squamous cell carcinoma. Oral Oncol, 46(11), 814-817.

Lee, J., Romero, R., & Dong, Z. (2012). Glycogen phosphorylase isoenzyme BB plasma concentration is elevated in pregnancy and preterm preeclampsia. Hypertension, 59(2),274-282.

Liu, SC., Sauter, ER., & Clapper, ML.(1998). Markers of cell proliferation in normal epithelia and dysplastic leukoplakias of the oral cavity. Cancer Epidemiol Biomark Prev, 7(7),597-603.

Morifuji, M., Taniguchi, S., & Sakai, H.(2000). Differential expression of cytokeratin after orthotopic implantaion of newly established human tongue cancer cell lines of fined metastatic ability. Am J Pathol, 156(4),1317-1326.

Nakanishi, Y., Ochiai, A., & Shimoda, T.(1997). Epidermization in the esophageal mucosa: unusual epithelial changes clearly detected by Lugol's staining. Am J Surg Pathol, 21(5),605-609.

Newgard, CB., Hwang, PK., & Fletterick, RJ.(1989). The family of glycogen phosphorylases: structure and function. Crit Rev Biochem Mol Biol, 24(1),69-99.

Ogawa, T., Washio, J., & Takahashi, T.(2014). Glucose and glutamine metabolism in oral squamous cell. Oral Surg Oral Med Oral Pathol Oral Radiol1, 118(2),218-225.

Ohta, K., Ogawa, I., & Ono, S.(2010). Histopathological evaluation including cytokeratin 13 and Ki-67 in the border between Lugol-stained and -unstained areas. Oncol Rep, 24(1),9-14.

Ritterson, Lew, C., Guin, S., & Theodorescu, D.(2015). Targeting glycogen metabolism in bladder

cancer. Nat Rev Urol, 12(7),383-391.

Roach, PJ., Cheng, C., & Huang, D.(1998). Novel aspects of the regulation of glycogen storage. J Basic Clin Physiol Pharmacol, 9(2-4),139-151.

Shimane, T., Kobayashi, H., & Takeoka, M.(2013). Clinical significance of apoptosis-associated speck-like protein containing a caspase recruitment domain in oral squamous cell carcinoma. Oral Surg Oral Med Oral Pathol Oral Radiol, 115(6),799-809.

Shimizu, Y., Tsukagoshi, H., & Fujita, M.(2001). Endoscopic screening for early esophageal cancer by iodine staining in patients with other current or prior primary cancers. Gastrointest Endosc, 53(1),1-5.

Skurat, AV., & Roach, PJ.(1995). Phosphorylation of sites 3a and 3b (Ser640 and Ser644) in the control of rabbit muscle glycogen synthase. J Biol Chem, 270(21),12491-12497.

Xiao, T., Kurita, H., & Shimane, T.(2013). Vital staining with iodine solution in oral cancer: iodine infiltration, cell proliferation, and glucose transporter 1. Int J Clin Oncol, 18(5),792-800.

Yu, JP., Ladapo, J., & Whitman, WB.(1994). Pathway of glycogen metabolism in Methanococcus maripaludis. J. Bact, 176(2);325-332.

Zois, CE., Favaro, E., & Harris, AL.(2014). Glycogen metabolism in cancer. Biochem Pharmacol, 92(1),3-11.

Figure legends

Fig. 1. Specimens collection

(Left upper panel) A photograph of iodine vital staining of the tongue.

(Right upper panel) Specimens containing both iodine-stained and unstained mucosal tissue were obtained.

(Left lower panel) Various layers were stained with iodine solution and immunohistochemical techniques.

Fig. 2. Serial histopathological sections of a surgical margin specimen including both iodine positive (normal) and negative (severe dysplastic) area

The arrowhead indicates the boundary between the iodine-stained and unstained areas.

(a) No staining: a clear boundary was seen between the unstained area (left) and iodine-stained area (right).

(b) Hematoxylin and eosin (H&E) staining: two distinct histopathological expression patterns that closely mirrored those produced by iodine staining were seen.

(c) Periodic acid–Schiff (PAS) staining: large numbers of glycogen granules were observed in the iodine-positive epithelium, but no such granules were seen in the iodine-negative epithelium.

(d) and (e) Immunohistochemical expression for (d) p53,and (e) Ki67.

In figures (d), and (e), higher cell positivity were seen in the unstained epithelia than in the stained epithelia.

(a)–(e) Magnification: ×150

Fig. 3. Comparison of the cell positivity rates for each epithelial layer between the iodine-stained and unstained areas

(a) and (b): glycogen synthase (GS) staining, (C) and (d): phospho-glycogen synthase (PGS) staining, (e) and (f): glycogen phosphorylase isoenzyme BB (GPBB) staining, and (g): glucagon-like peptide-1 (GLP-1) staining.

(a), (c), (e), and (g) Magnification: ×150.

In figures (a) and (c), similar cell positivity patern were observed in the unstained epithelia and stained epithelia.

In figure (e), higher cell positivity was seen in the unstained epithelia than in the stained epithelia.

In figure (g), no GLP-1 expression was detected.

Iodine (+), iodine-positive area; iodine (-), iodine-negative area (*P<0.01, Wilcoxon signed-rank test)

Fig. 4 Cell immunofluorescence

A: Immunofluorescence detected using an antibody against GS

(a) NHEK, (b) HaCaT, (c) SAS, (d) HSC-2, (e) HSC-3, (f) SQUU-A, (g) SQUU-B, and (h) Ca9-22

B : Immunofluorescence detected using an antibody against GPBB

(a) NHEK, (b) HaCaT, (c) SAS, (d) HSC-2, (e) HSC-3, (f) SQUU-A, (g) SQUU-B, and (h) Ca9-22

The cancer cells exhibited significantly stronger GPBB-related fluorescence than the normal cells.

C: Quantitative analysis of the fluorescence intensity (Alexa Fluor 488) produced by antibodies against GS and GPBB performed using the Leica Confocal Software (LCS) [A.U. = arbitrary units].

GPBB was expressed at significant greater levels than GS in the OSCC cells (GS vs GPBB; Wilcoxon signed-rank test: NHEK:NS, all OSCC cell lines: $P<0.01$).

Fig. 5. Western blotting and real-time PCR analysis of GS and GPBB expression in OSCC cell lines and normal keratinocytes

A: Western blot analysis (A).

GS and GPBB expression were observed in most cell lines. However, stronger GPBB expression was seen in the cancer cell lines than in the NHEK.

B & C: Real-time PCR analysis for GS (B) and GPBB (C)

Real-time quantitative PCR revealed that although similar GS expression levels were seen in the

normal and cancer cells, higher mRNA expression levels of GPBB in the 6 OSCC cell lines than in the NHEK (NHEK vs each OSCC cell lines; Wilcoxon signed-rank test: SAS, HSC-2, and HSC-3: $P<0.05$, SQUU-A, SQUU-B, and Ca9-22: $P<0.01$).

Fig. 6. Glycogen metabolism pathways

Glycogenesis produces glycogen from glucose. Glycogenolysis involves the breakdown of glycogen back to glucose. Glycogenesis and glycogenolysis occur in the cell cytoplasm.

Table 1. Patients' clinical and histopathological features (n = 21)

Table 2. Specific primers used for the real-time PCR

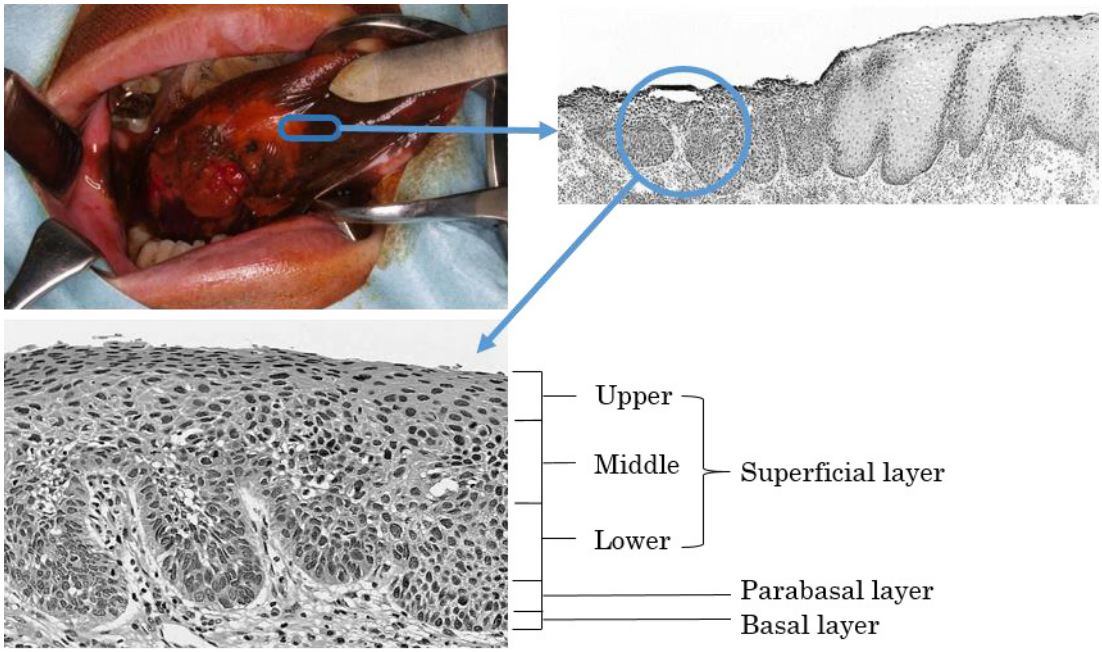

Fig. 1.

Specimens collection.(Left upper panel) A photograph of iodine vital staining of the tongue.(Right upper panel) Specimens containing both iodine-stained and unstained mucosal tissue were obtained. (Left lower panel) Various layers were stained with iodine solution and immunohistochemical techniques.

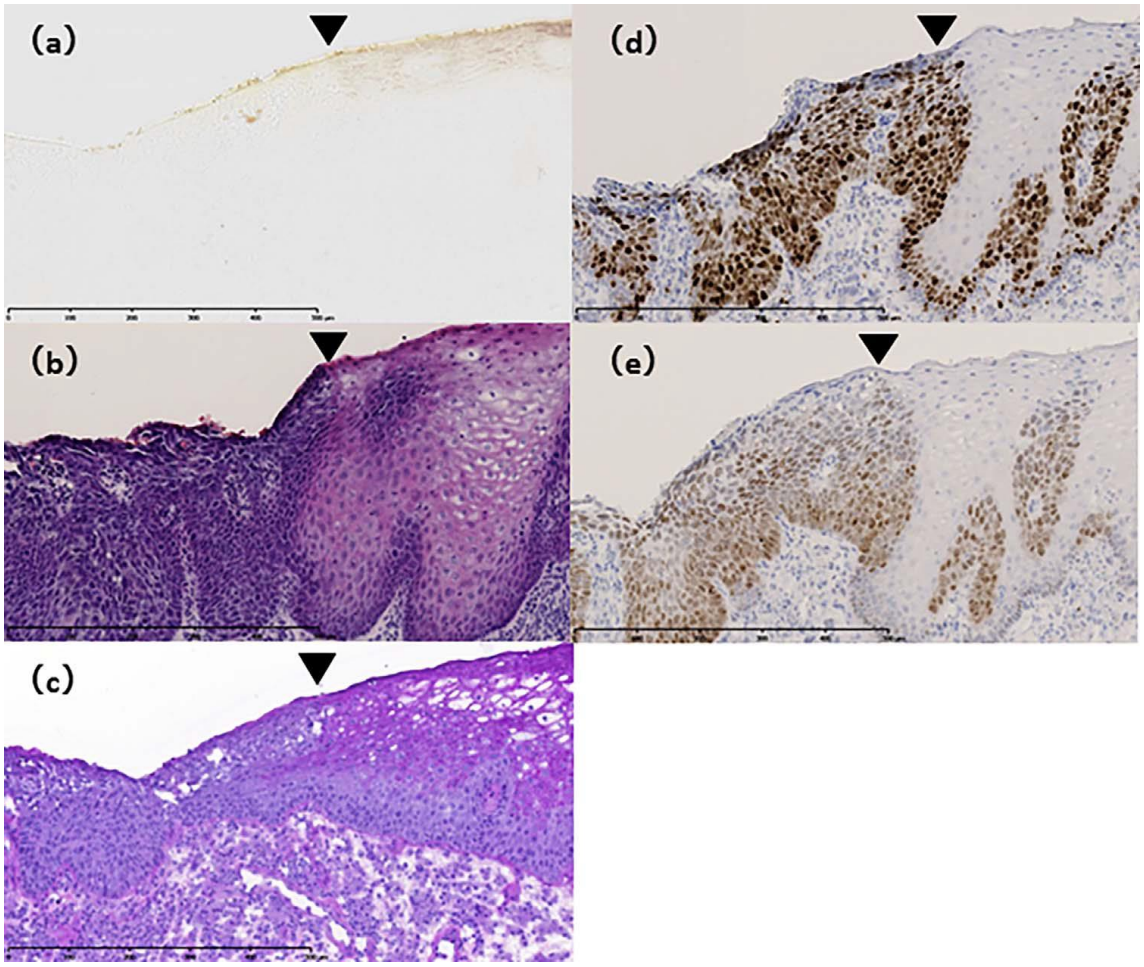

Fig. 2.

Serial histopathological sections of a surgical margin specimen including both iodine positive (normal) and negative (severe dysplastic) area. The arrowhead indicates the boundary between the iodine-stained and unstained areas.

(a) No staining: a clear boundary was seen between the unstained area (left) and iodine-stained area (right).

(b) Hematoxylin and eosin (H & E) staining: two distinct histopathological expression patterns that closely mirrored those produced by iodine staining were seen.

(c) Periodic acid–Schiff (PAS) staining: large numbers of glycogen granules were observed in the iodine-positive epithelium, but no such granules were seen in the iodine-negative epithelium.

(d) and (e) Immunohistochemical expression for (d) p53,and (e) Ki67. In figures (d), and (e), higher cell positivity were seen in the unstained epithelia than in the stained epithelia.

(a)–(e) Magnification: ×150

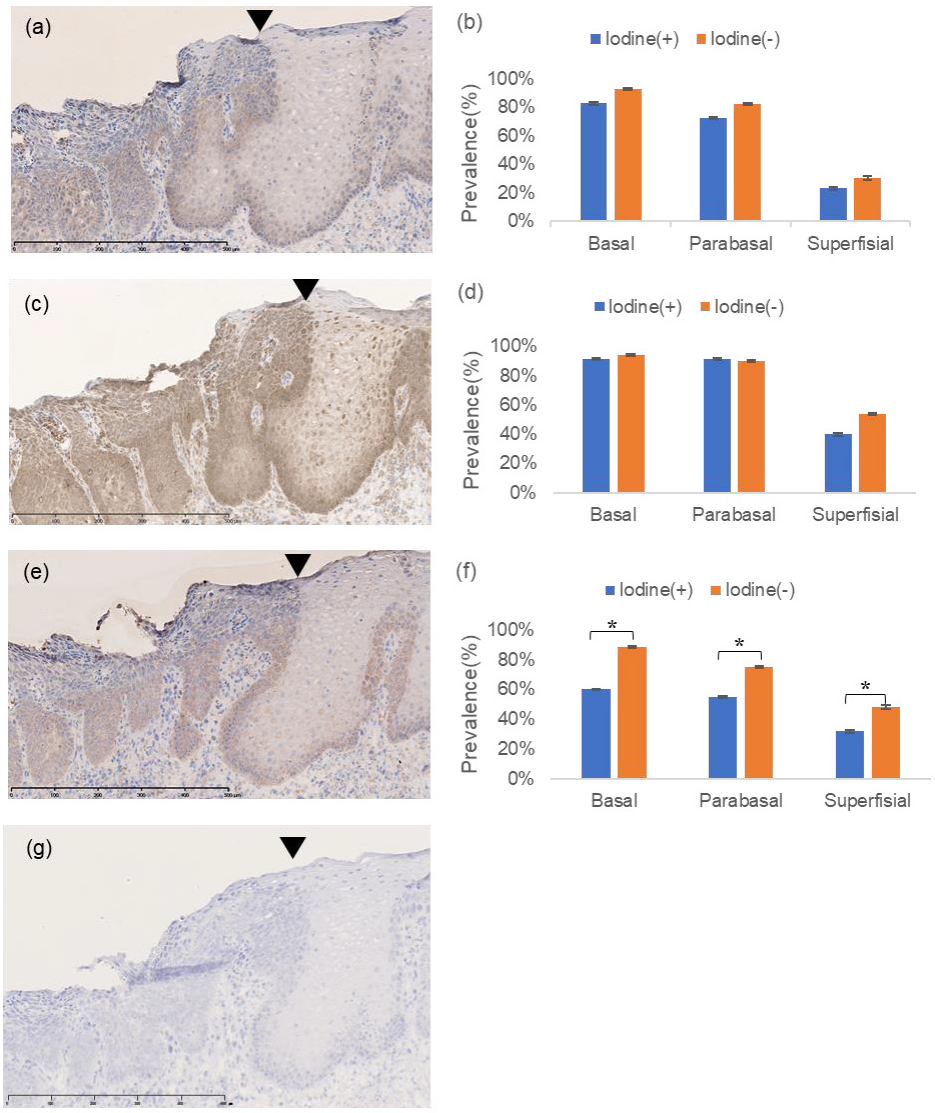

Fig. 3. Comparison of the cell positivity rates for each epithelial layer between the iodine-stained and unstained areas.

(a) and (b): glycogen synthase (GS) staining, (c) and (d): phospho-glycogen synthase (PGS) staining, (e) and (f): glycogen phosphorylase isoenzyme BB (GPBB) staining, and (g): glucagon-like peptide-1 (GLP-1) staining.

(a), (c), (e), and (g) Magnification: ×150.

In figures (a) and (c), similar cell positivity patern were observed in the unstained epithelia and stained epithelia.

In figure (e), higher cell positivity was seen in the unstained epithelia than in the stained epithelia.

In figure (g), no GLP-1 expression was detected. Iodine (+), iodine-positive area; iodine (–), iodinenegative area (*P < 0.01, Wilcoxon signed-rank test)

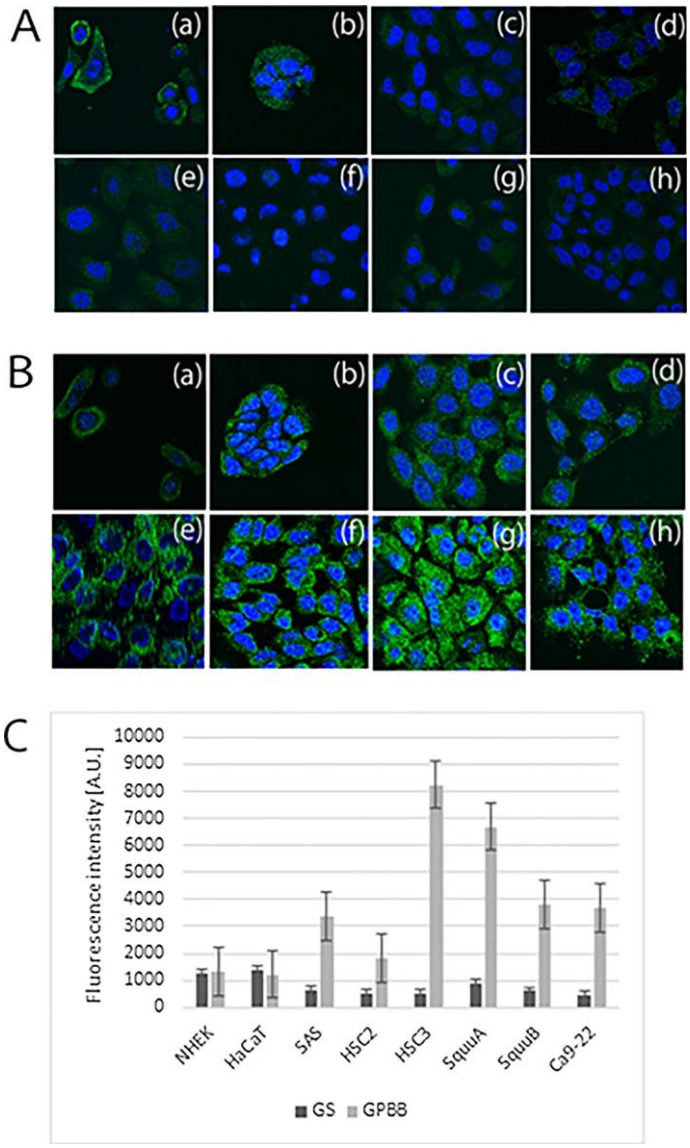

Fig. 4. Cell immunofluorescence.

A: Immunofluorescence detected using an antibody against GS. (a) NHEK, (b) HaCaT, (c) SAS, (d) HSC-2, (e) HSC-3, (f) SQUU-A, (g) SQUU-B, and (h) Ca9-22

B: Immunofluorescence detected using an antibody against GPBB. (a) NHEK, (b) HaCaT, (c) SAS, (d) HSC-2, (e) HSC-3, (f) SQUU-A, (g) SQUU-B, and (h) Ca9-22

The cancer cells exhibited significantly stronger GPBB-related fluorescence than the normal cells.

C: Quantitative analysis of the fluorescence intensity (Alexa Fluor 488) produced by antibodies against GS and GPBB performed using the Leica Confocal Software (LCS) [A.U. = arbitrary units]. GPBB was expressed at significant greater levels than GS in the OSCC cells (GS vs GPBB; Wilcoxon signedrank test: NHEK:NS, all OSCC cell lines: $P < 0.01$).

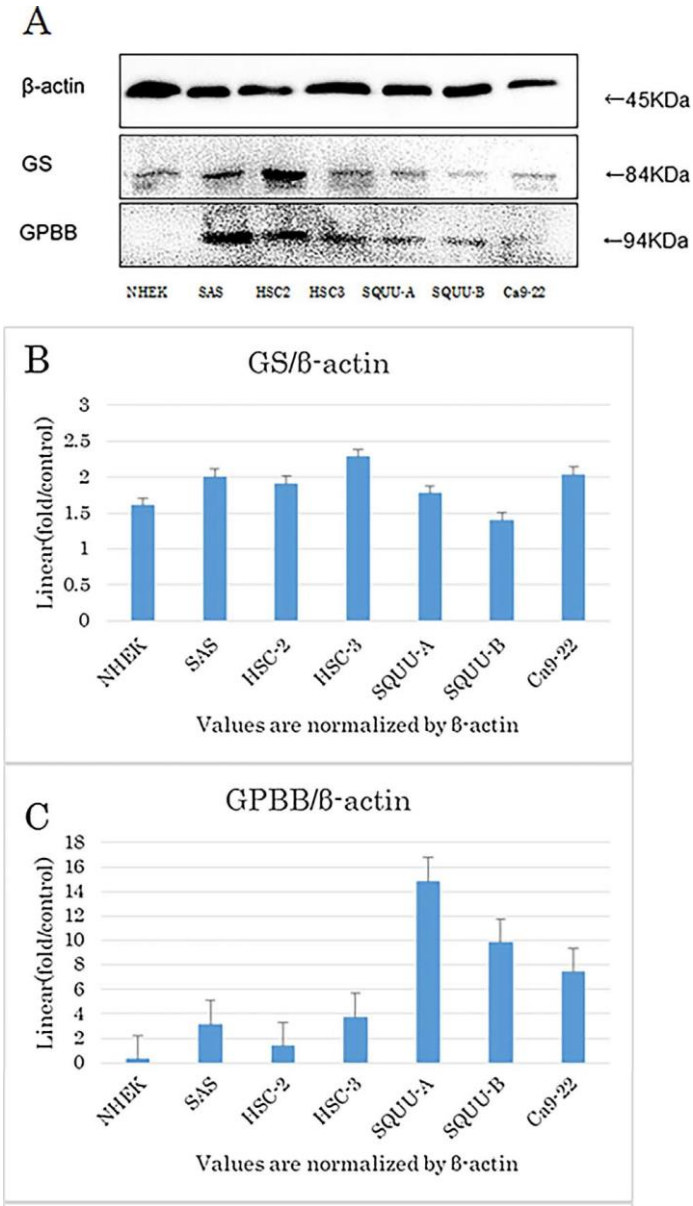

Fig. 5. Western blotting and real-time PCR analysis of GS and GPBB expression in OSCC cell lines and normal keratinocytes.

A: Western blot analysis (A).

GS and GPBB expression were observed in most cell lines. However, stronger GPBB expression was seen in the cancer cell lines than in the NHEK.

B & C: Real-time PCR analysis for GS (B) and GPBB (C).

Real-time quantitative PCR revealed that although similar GS expression levels were seen in the normal and cancer cells, higher mRNA expression levels of GPBB in the 6 OSCC cell lines than in the NHEK (NHEK vs each OSCC cell lines; Wilcoxon signed-rank test: SAS, HSC-2, and HSC-3: $P < 0.05$, SQUU-A, SQUU-B, and Ca9-22: $P < 0.01$).

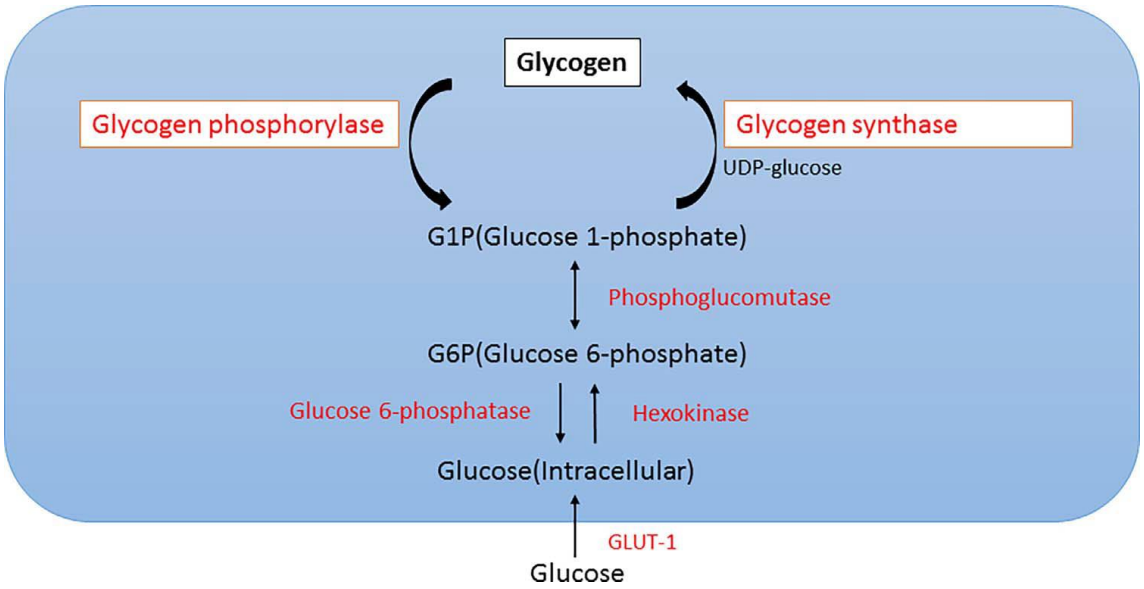

Fig. 6. Glycogen metabolism pathways.

Glycogenesis produces glycogen from glucose. Glycogenolysis involves the breakdown of glycogen back to glucose. Glycogenesis and glycogenolysis occur in the cell cytoplasm.

Table1. Clinical and histopathological features and patients (n = 21)

Characteristics	Number
Gender	
Male	11
Female	10
Age(years)	
Range	26-92
Median	70
Primary site	
Tongue	12
Floor of mouth	1
Gingival	8
Histopathological diagnosis	
Squamous cell carcinoma	21

Table2. Specific primer for real-time PCR

Gene	*Sense primer*	*Antisense primer*
β -actin	5'-GGACTTCGAGCAAGAGATGG-3'	5'-GTGGATGCCACAGGACTCCAT-3'
GS	5'-ATCGAGGCACAGCACTTG-3'	5'-GGCGATAAAGAAGTATAAGGTCTTG-3'
GPBB	5'-CCATCTATCAGTTGGGGTTAGACT-3'	5'-CTGCCAGCCATTGACAATC-3'